Flight X-ray CCD Selection for the AXAF CCD Imaging Spectrometer

M. Pivovaroff[1], S. Kissel[1], M. W. Bautz[1], G.Y. Prigozhin[1], T. Isobe[1], J. Woo[1], J.A. Gregory[2]

[1]Massachusetts Institute of Technology–Cambridge, Massachusetts 02139
[2]MIT Lincoln Laboratories–Lexington, Massachusetts 02173

ABSTRACT

As part of our program to select and calibrate flight-quality, X-ray CCD detectors for the AXAF CCD Imaging Spectrometer, we have developed efficient detector screening methods. Our screening protocol, which measures device-level performance parameters (including noise, dark current and charge transfer efficiency) as well as X-ray spectral resolution in the 0.3 - 6 keV band, allows us quickly to identify which of the $>$ 30 flight candidate detectors warrant the expenditure of severely limited time available for calibration. The performance criteria used to rank devices are discussed, and the details of the measurement methods are presented. Summary results of the screening measurements are presented for a large sample of devices, and detailed data on selected devices are described. We find that the performance variations among the sample of flight devices to be relatively small but significant.

KEYWORDS: ACIS, AXAF, calibration, CCD

1 Introduction

NASA's Advanced X-Ray Astrophysics Facility (AXAF) is scheduled for launch in September, 1998. The AXAF telescope employs Wolter type I grazing optics and has two focal plane instruments, the microchannel plate High Resolution Camera (HRC) and a CCD based instrument, the AXAF CCD Imaging Spectrometer (ACIS). AXAF also has two grating instruments, the High Energy Transmission Grating (HETG) and the Low Energy Transmission Grating (LETG).[1,2] The ACIS instrument consists of two separate detector arrays, ACIS-I and ACIS-S. ACIS-I is a 2x2 array of CCDs intended for imaging. ACIS-S is a 1x6 array of CCDs intended for use with the HETG to do spectroscopy.[3]

The scientific objectives of the program demand thorough calibration of each CCD placed in the ACIS-I and the ACIS-S. As complete characterization of a single device heavily taxes personnel and laboratory resources, calibration of each of the more than thirty flight quality CCDs becomes infeasible. In response to these constraints, we have developed screening techniques that allow us to determine which CCDs deserve a complete calibration.

In this paper, we describe the measurements that comprise the screening protocol, including determination of device-level performance parameters and the spectral resolution in the .3 - 6 keV band. In addition to discussing the motivation for the acceptance criteria, we summarize the screening results and present representative performance data.

2 ACIS Detectors

The ACIS instrument uses MIT Lincoln Laboratory CCID 17 Devices.[4] These CCDs consist of a 1024 x 1026 pixel imaging section, with a separate 1024 x 1026 shielded frame store region. The pixels are 24μm square, and when coupled with the focusing optics, will provide resolution of 0.5 arcseconds. The frame store for these devices has a novel architecture, with two separate sections that feed into two independent serial registers (see Figure 1). This design permits charge to be clocked in either direction and makes possible non-standard readout configurations. For example output nodes A and B can be both be readout through output A, while nodes C and D are both readout through C (AC mode).[4]

Both front-illuminated (incident photons pass through the gate structure) and back-illuminated (incident photons incident directly into the depleted silicon) devices have been made for ACIS. Back-illuminated devices (BI) offer the advantage of higher quantum efficiency at lower energies, but have significantly lower spectral resolution than the front-illuminated (FI) devices.[5]

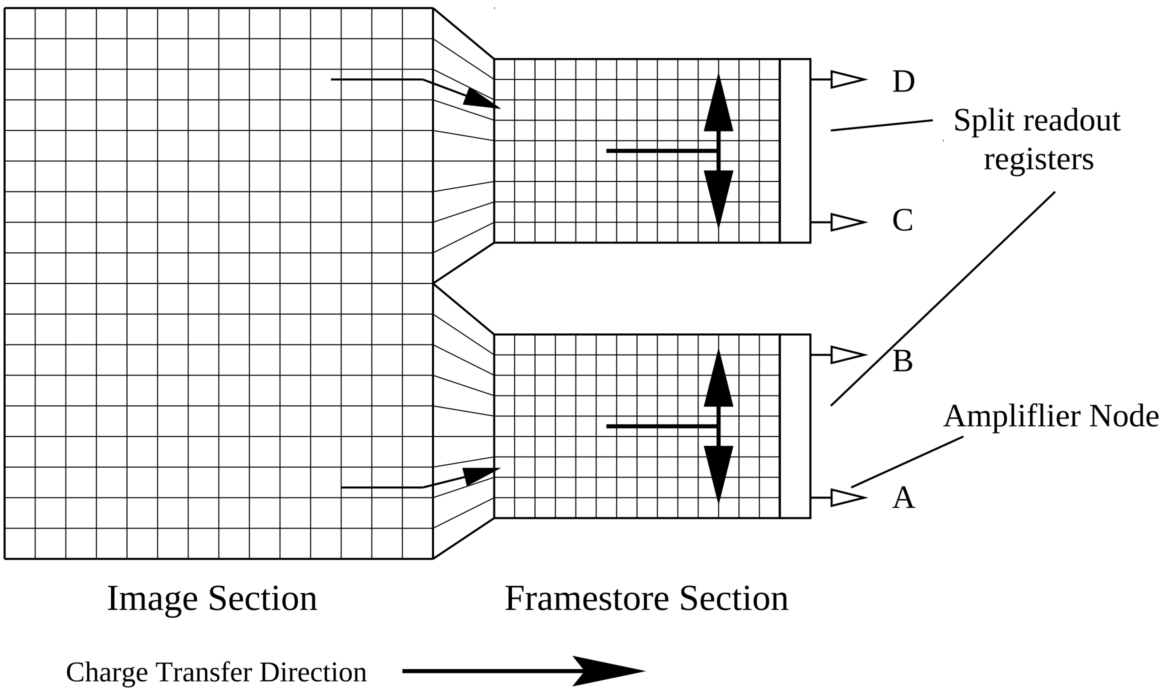

Figure 1: Schematic of CCID 17

3 Screening Protocol

3.1 Initial Inspection

Prior to shipment, MIT Lincoln Laboratories checks the output nodes of each device for functionality and operates the devices at -40 C to verify cosmetic quality. Once received at MIT CSR, the CCD is installed in a vacuum chamber, the chamber is evacuated to a pressure of $1 \cdot 10^{-6}$ torr, and the device is cooled to -120 C. The device is then exposed to an ^{55}Fe source to ensure that it can detect X-rays and has no gross defects.

3.2 Tuning

Before the screening process begins, proper optimization of the CCD's clock voltages must occur. The CCD biases which have the greatest effect on device performance are drain bias applied to each of the four on-chip MOSFET amplifiers. Indeed, we find that excellent device performance is achieved with standard set biases for the charge transfer and reset clock voltages for all devices. Thus, only the drain biases must be adjusted for each CCD. This flexibility allows us to set charge transfer clock levels to maximal depletion depth. Bias (source-free) and X-ray data (again using an ^{55}Fe source) are taken over a wide range of clock voltages. The Mn K_α and Mn K_β lines provide a gain conversion and allow determination of noise in electron units (see Section 3.4). During the subsequent screening and calibration measurements, the CCD's clocks are operated at the voltages that produced the lowest RMS noise.

3.3 Data Acquisition

3.3.1 CCD Readout Modes

Nominal operation of both ACIS-I and ACIS-S involves reading out each CCD through four output nodes in parallel in a timed exposure mode (time = 3.227 seconds for standard mode). During the course of the AXAF mission, however, other modes with different exposure times may be preferred for particular types of measurements. Continuous read-out modes (charge is continually clocked from the device) will be useful for observations where precision timing is important. Summation modes (blocks of pixels summed together and read out as a single pixel) exist to avoid pile up during observation of bright sources. Another mode variation allows the entire device to be readout through two output nodes (AC or BD). Reading out only a sub-array of the device reduces the integration time and permits observation of brighter sources. In total we examine eight different operational modes during the screening process. Table 1 lists each mode and briefly describes it.

3.3.2 Required Data Sets

Characterization of each readout mode requires several measurements. Using a reflection grating monochromator, the CCD is illuminated with monochromatic photons at the energy corresponding to the oxygen K_α line (525 eV) and the aluminum K_α line (1.49 keV). The device is also exposed to Mn K_α and K_β lines produced by an ^{55}Fe source. These three measurements provide a determination of charge transfer inefficiency (CTI), energy scale, and spectral resolution over a broad energy range between .5 - 6 keV. Finally, dark current data are taken at a range of integration times, and a number of bias frames are taken. This procedure allows calculation of the dark current present in the CCD.

A typical measurement begins by configuring the CCD to perform in a specific mode by proper programming of the CCD clock sequencing electronics. For the three spectral resolution/CTI data sets, flux levels are checked and adjusted to maximize incident flux consistent with acceptable pile-up. We then collect enough data to ensure that $1 \cdot 10^5$ photons are incident on each CCD quadrant. Bias data is taken immediately preceding the collection of X-ray data. Finally, the dark current data is taken. Table 2 shows the typical measurements made for each mode and the number of frames obtained.

Operating Mode	Description	Exposure Time
standard	minimum exposure time for full frame readout	3.277 sec
first 100	similar to standard, but only the first 100 rows read out	0.542 sec
last 100	similar to standard, but only the last 100 rows read out	0.579 sec
AC	nodes A and B read out through A;	
	nodes C and D read out through C	5.906 sec
BD	nodes A and B read out through B;	
	nodes C and D read out through D	5.906 sec
continuous 1x1	Imaging area parallel clocks operate continually	continuous
continuous 1x2	Charge continually clocked through device;	
	two neighboring vertical pixels summed together	continuous
2X2	a square of four neighboring pixels summed	
	together and readout as one pixel	1.114 sec

Table 1: Description of Readout Modes

Mode	Number of Frames			
	O K_α	Al K_α	^{55}Fe	Dark Current
standard	100	100	100	40
first 100	800	800	800	40
last 100	800	800	800	40
AC	80	80	80	40
BD	80	80	80	40
continuous 1x1	100	100	100	none
continuous 1x2	100	100	100	none
2x2	300	300	300	40

Table 2: Data Sets for Each Readout Mode

3.4 Data Analysis

Analysis starts with the ^{55}Fe data set. The code subtracts bias levels and corrects for drift in the overclocks before using ASCA event detection and grading algorithms to find events. Event "grades" are assigned on the basis of the spatial charge distribution in a 3x3 pixel neighborhood surrounding each event. Grades are used to select events with well-collected charge. Overclocks are thirty additional serial transfers that occur after each row has been read out. Changes in overclock levels indicate drift in the electronics. The event list is then searched to locate hot columns (defined as a column with a bias level 50 e$^-$ greater than the median level), hot pixels (defined as a pixel with a bias level 50 e$^-$ greater than the median bias level), and bad columns (defined as columns with low X-ray detection efficiency). If any hot columns or hot pixels are found, events from these columns are removed from the ^{55}Fe data and subsequent data sets.

With a properly corrected data set, noise, CTI, dark current, and spectral resolution can be calculated. Noise is determined by computing the pixel-by-pixel difference of two bias frames. A Gaussian is fit to the histogram of this difference frame. The standard deviation of this Gaussian is taken to be $\sqrt{2}$ time the RMS system noise.

Histograms are made of the graded events and used for CTI and spectral resolution measurements. CTI is calculated by plotting pulse height values versus row number (parallel CTI measurements) or column number (serial CTI measurements), fitting a line of the form: $ph(y) = ph(0) + \delta \cdot y$ to the data, and equating CTI to $\delta / ph(0)$. Then a Gaussian is fit to the Mn k_α line to determine the spectral resolution and energy scale of the CCD at 5.9 keV. Each of these processing steps is repeated for the aluminum and oxygen data sets in order to provide device-level performance information over a broad energy band (0 to 5.9 keV). Section 5.2 contains sample data and plots.

Dark current is calculated for modes with exposure times that can be varied. An average bias frame is calculated from the dark current data taken at the normal exposure time (3.277 seconds for standard mode). After the data has been bias subtracted and overclock corrected, an average pixel value is determined for each dark frame from a histogram of the pixels in the image section. A linear relationship of the form: $m(t) = a + b(t - 3.277)$ is fit to the data, where b is the mean dark current in adu/pixel/sec and $m(t)$ is the mode bias value for a frame with integration time t. This value is converted from engineering units to electron/pixel/sec using the gain values determined from the ^{55}Fe measurements.

When the analysis has finished, the code processes the results and creates a summary sheet that details the CCD's performance and determines if it meets the acceptance criteria. This report presents all the relevant information in a readily digestible form and provides the ACIS team with the information needed to decide whether to fully calibrate a particular device. Figure 2 is the screening report for device c17-185-3. Besides displaying the measured quantities in tables, the summary sheet also lists the acceptance criteria and then decides if the device passed (P) or failed (F). The entire data acquisition and analysis process can be completed in about four hours.

Figure 2: Screening Report for device c17-185-3

Screening Report (FI) for c17-185-3 [T=-120.0 C]
(data_dir = /nfs/rico/d7/w185c3/23Jan96)
(output_dir = /ohno/da/Screen/c17-185-3/23Jan96/screen)
Fri Apr 5 14:56:38 EST 1996

Event Threshold = 100 ADU
Split Threshold:
Node0: 13
Node1: 13
Node2: 12
Node3: 13
Grade: cti(0-7); spec_resol(0,2-4); gain(0,2-4)

<Readout Noise (noise[im]+d < 5 e-)>

Node(im)	Noise(electron)	Node(oc)	Noise(electron)	Test
c0im	2.133 +/- 0.002	c0oc	2.084 +/- 0.007	P
c1im	2.735 +/- 0.003	c1oc	2.672 +/- 0.009	P
c2im	1.885 +/- 0.002	c2oc	1.812 +/- 0.006	P
c3im	1.904 +/- 0.002	c3oc	1.761 +/- 0.006	P

<Parallel CTI [Fe55 at 5.9 keV] (< 5e-6)>

Node	CTI	Test
c0	1.06836e-07 +/- 3.37265e-07	P
c1	6.86257e-08 +/- 3.38151e-07	P
c2	-2.11046e-07 +/- 3.28082e-07	P
c3	-1.13295e-07 +/- 3.49976e-07	P

<Parallel CTI [O_k at 0.525 keV] (< 5e-5)>

Node	CTI	Test
c0	8.01778e-06 +/- 1.87914e-06	P
c1	1.90632e-06 +/- 2.00573e-06	P
c2	7.50403e-06 +/- 1.80480e-06	P
c3	5.86082e-06 +/- 2.05938e-06	P

<Serial CTI [Fe55 at 5.9 keV] (< 1e-5)>

Node	CTI	Test
c0	-3.91665e-06 +/- 1.33823e-06	P
c1	-1.53416e-06 +/- 1.33965e-06	P
c2	-3.74164e-07 +/- 1.30727e-06	P
c3	1.37959e-06 +/- 1.35999e-06	P

<Mean Dark Current (< 0.3 e/pix/s)>

Node	Dark Current (e/pix/s)	(95% uplimit)	Test
c0	0.039285 +/- 0.000205	(0.220000)	P
c1	0.034888 +/- 0.000254	(0.260000)	P
c2	0.029906 +/- 0.000211	(0.220000)	P
c3	0.070693 +/- 0.000202	(0.260000)	P

<Spectral Resolution [O_k at 0.525 keV] (FI:< 70eV)>

Node	FWHM(eV)	Test
c0	44.3276 +/- 0.412155	P
c1	48.4973 +/- 0.455946	P
c2	43.8841 +/- 0.412187	P
c3	42.9952 +/- 0.463458	P

<Spectral Resolution [Al_k at 1.487 keV] (FI:< 100eV)>

Node	FWHM(eV)	Test
c0	67.4721 +/- 0.344109	P
c1	69.5684 +/- 0.367777	P
c2	67.093 +/- 0.363496	P
c3	66.5883 +/- 0.385113	P

<Spectral Resolution [Fe55 at 5.898 keV] (< 165eV)>

Node	FWHM(eV)	Test
c0	128.472 +/- 0.716822	P
c1	129.882 +/- 0.726135	P
c2	127.188 +/- 0.706473	P
c3	127.231 +/- 0.729545	P

<Gain>

Node	O_Gain(eV/ADU)	Al_Gain(eV/ADU)	Fe_Gain(eV/ADU)
c0	4.07735 +/- 0.00187521	4.04416 +/- 0.000548207	4.05378 +/- 0.000287081
c1	4.14169 +/- 0.00204711	4.10557 +/- 0.000597824	4.11283 +/- 0.000293099
c2	4.53748 +/- 0.00206868	4.50461 +/- 0.000644549	4.508 +/- 0.00031659
c3	4.22243 +/- 0.00215265	4.1942 +/- 0.000632717	4.21641 +/- 0.000302656

<Hot Pixels>
0 hotpixel
0 hotcol
0 hotpixel not in hotcol
<Bad Columns>
0 badcol

4 Acceptance Criteria

4.1 Performance Parameters

4.1.1 Noise

System noise directly affects spectral resolution, especially at the lowest X-ray energies. This dependence is illustrated in Table 3. We have adopted a requirement of 5 e^- RMS, as a level which is readily achievable, and which minimizes the contribution of system noise to energy resolution. At this noise level, photoionization statistics, rather than readout noise, is the dominant contribution to spectral resolution for energies above 500 eV.

4.1.2 Charge Transfer Inefficiency (CTI)

CTI is the measure of how efficiently a CCD transfers a charge packet from the image array to the output node. Devices with high CTI will not transfer all of the photo electrons associated with an X-ray event to the output node. This charge loss results in position dependent energy scale which in turn leads to degradation in the spectral resolution for the entire device. These undesirable effects can be negated by demanding that the CTI fall below a critical level. We have chosen a threshold of $5 \cdot 10^{-6}$, measured at 5.9 keV, for parallel CTI. At this level, CTI makes no measurable contribution to device energy resolution.

4.1.3 Spectral Resolution

For front-illuminated (FI) CCDs the spectral resolution of a single pixel event is limited by the RMS noise of the system and the Fano factor of silicon. The theoretical prediction for resolution is given by the well known relation:

$$FWHM = 2.35 \cdot \epsilon \sqrt{N^2 + \frac{EF}{\epsilon}}$$

where N is the RMS noise in electrons, ϵ is the energy needed to create one electron-hole pair (3.65 eV/pair), F is the Fano factor for silicon (F=.12, and E is the photon energy in eV).[6] The thinning process used in fabricating back-illuminated (BI) CCDs results in poorer spectral response, forcing a relaxation of the threshold values for BI devices. Table 3 lists the acceptance criteria for FI and BI CCDs and theoretical limits for single pixel events in FI devices.

	BI	FI			
			Theoretical Limits Single Pixel Events		
Photon Energy	Acceptance Criteria	Acceptance Criteria	N=2 e^-	N=4 e^-	N=6 e^-
525 eV	120 eV	70 eV	40 eV	49 eV	63 eV
1487 eV	120 eV	100 eV	62 eV	69 eV	79 eV
5898 eV	165 eV	165 eV	121 eV	124 eV	130 eV

Table 3: Spectral Resolution Values from .5 - 6 keV for Single Pixel Events

4.1.4 Dark Current

Dark current is the measure of thermally excited free charge in the CCD. The screening is conducted at the expected flight temperature of -120 C, and at these temperatures the dark current is so low that is has no significant effect on the performance of the CCD. The acceptance criteria requires devices to have dark currents below .3 electrons/pixel/second.

4.1.5 Cosmetics

Cosmetics is a blanket term used to describe device morphology, including hot columns, bad columns, hot pixels, and edge glow (contiguous regions of hot pixels along the edge of the chip created when the silicon wafer is cut). A CCD with gross defects (regions on order of 100 pixels square) is immediately removed from consideration. A device with a few bad or hot columns or tens of hot pixels that meets the other screening criteria is fully calibrated. The acceptance criteria for cosmetics is that a CCD have fewer than twenty total defective columns, with no greater than ten defective columns occurring in any quadrant.

5 Results

5.1 Summaries

Table 4 lists the devices (and their performance parameters) that meet the minimum screening criteria. In an attempt to simplify the presentation of the results, we do not include data for each output node, but rather give either an upper limit or a range of values.

Upon inspection two features become quite obvious: 1) The BI devices have much poorer energy resolution and higher CTI than the FI devices. Due to their increased quantum efficiency at low energies, BI devices are still being considered as potential ACIS-S detectors.[5] 2) The first ten FI CCDs (w129c2-w168c2) have noise values a few electrons higher than the other CCDs. This property is actually due to the electronics used and is not inherent to the devices. Flight-like electronics, with better performance than standard laboratory electronics, were used starting with device w163c1.

Device(FI/BI)	Noise (e^- RMS)	Dark Current (e^-/pix/s @ -120C)	PCTI ($\times 10^{-6}$ @5.9 keV)	Spectral Resolution (eV, FWHM; full-frame) 525 eV	1.5 keV	5.9 keV
w147c3 (BI)	2.7 - 2.9	0.08 - 0.2	1.5 - 2.5	92 - 103	99 - 119	140 - 151
w140c4 (BI)	3.0 - 3.0	< 0.01	22 - 27	147- 156	165 - 186	240 - 290
w134c4 (BI)	2.8 - 3.0	0.01 - 0.02	11 - 15	117 - 121	112 - 117	179 - 203
flight criteria (BI)	< 5	< 0.3	< 50	120	120	165
w129c2 (FI)	2.6 - 3.7	< 0.01	< 1	47 - 57	69 - 76	129 - 135
w78c1 (FI)	2.8 - 3.0	< 0.01	< 1	48 - 51	69 - 73	130 -137
w97c1 (FI)	2.7 - 3.4	< 0.01	1 - 3	49 - 62	73 - 86	128 - 134
w157c1 (FI)	3.2 - 4.3	< 0.01	< 1	51 - 65	83 - 96	132 - 142
w157c2 (FI)	2.9 - 3.0	< 0.01	< 1	49 - 55	82 - 85	129 - 136
w158c2 (FI)	2.9 - 4.3	< 0.01	< 1 - 1.2	47 - 60	69 - 80	130 - 152
w158c4 (FI)	2.5 - 4.0	< 0.01	< 1	48 - 57	69 - 76	130 - 140
w159c1 (FI)	2.9 - 3.7	< 0.01	< 1	52 - 71	73 - 77	133 - 146
w163c3 (FI)	3.4 - 4.1	< 0.01	< 1	52 - 57	81 - 87	133 -145
w168c2 (FI)	3.2 - 4.0	< 0.01	< 1	52 - 57	88 - 91	132 - 138
w168c4 (FI)	2.2 - 2.5	< 0.01	< 1	46 - 48	80 - 82	129 - 132
w163c1 (FI)	2.4 - 2.7	< 0.01	< 1	47 - 47	68 - 70	130 - 134
w182c4 (FI)	3.0 - 3.9	0.02 - 0.05	< 1	50 - 54	70 - 74	129 - 134
w185c3 (FI)	1.9 - 2.7	< 0.03 - 0.07	< 1	43 - 48	67 - 69	127 - 130
w189c2 (FI)	2.9 - 4.1	< 0.01 - 0.17	< 1	48 - 56	76 - 81	130 - 136
w186c4 (FI)	2.8 - 4.5	< 0.01	< 1	48 - 63	71 - 81	130 - 137
w186c1 (FI)	2.7 - 3.8	< 0.01	< 1 - 2	50 - 58	71 - 78	131 - 145
w190c1 (FI)	2.3 - 2.5	< 0.01 - 0.02	< 1	45 - 46	68 - 69	129 - 131
w190c3 (FI)	2.2 - 2.2	0.02 - 0.03	< 1	43 - 45	68 - 70	127 - 130
w192c1 (FI)	2.0 - 2.1	0.07 - 0.02	< 1	44 - 44	66 - 67	127 - 129
w201c3 (FI)	1.9 - 2.1	0.04 - 0.06	< 1	44 - 45	68 - 69	129 - 130
w202c3 (FI)	1.9 - 2.0	0.02 - 0.05	< 1	42 - 43	66 -67	130 - 131
w203c2 (FI)	1.7 - 2.0	< 0.01	< 1	43 - 44	68 - 69	127 - 128
w183c3 (FI)	1.7 - 1.9	0.01- 0.09	< 1	42 - 48	70 - 74	129 - 132
w203c4 (FI)	1.8	0.01	< 1	43 - 44	79	127 - 129
w205c2 (FI)	1.9 - 2.0	0.01 - 0.02	< 1	43 - 44	68 - 69	127 - 130
w210c3 (FI)	2.2 - 2.3	0.01 - 0.02	< 1	44 - 45	69	134 - 136
w215c2 (FI)	1.8 - 2.0	0.01 - 0.02	< 1	42 - 43	67 - 71	125 - 130
w87c4 (FI)	1.8 - 2.0	0.01 - 0.02	< 1	43 - 48	68 - 69	128 - 130
average (FI)	2.6 - 2.8	.015 - .020	< 1	47 -49	73 - 75	131 - 134
flight criteria (FI)	< 5	< 0.3	< 1	70	100	165

Table 4: ACIS Flight CCD Screening Results

Most of the CCDs easily meet all the acceptance criteria, the only exception being a few devices that have noise levels that are less than one electron RMS from the threshold value. Comparing the spectral resolution measurements with the calculated values presented in Section 4.1.4 reveals that many devices are within 10 % of the theoretical limits. In practice, ranking of devices for calibration turned heavily on spectral resolution at 525 eV and on cosmetic properties. The most common cosmetic problem observed is the defective column. Typically, 2-3 defective columns are present, though a few devices have no defective columns, and one devices has as many as 15 column defects.

5.2 Sample Data

It is beyond the scope of this paper to discuss the performance of each device. Instead, we present data on one device that is representative of all flight quality CCDs. Figure 2 is the screening report for CCD c17-185-3 and contains all the measured device parameters.

Figure 3 shows the noise histogram and Gaussian fits for CCD c17-185-3. This device has the common trait of having lower noise in the over-clock region (OC in the plot) than in the image area (IM in the plot). The tails present in nodes c1 and c3 are representative of the shapes and sizes of non-Gaussian deviations that occur during noise characterization measurements. Generally, the histograms are accurately Gaussian over a range of four orders of magnitude.

Figure 3: Noise Histograms for c17-185-3

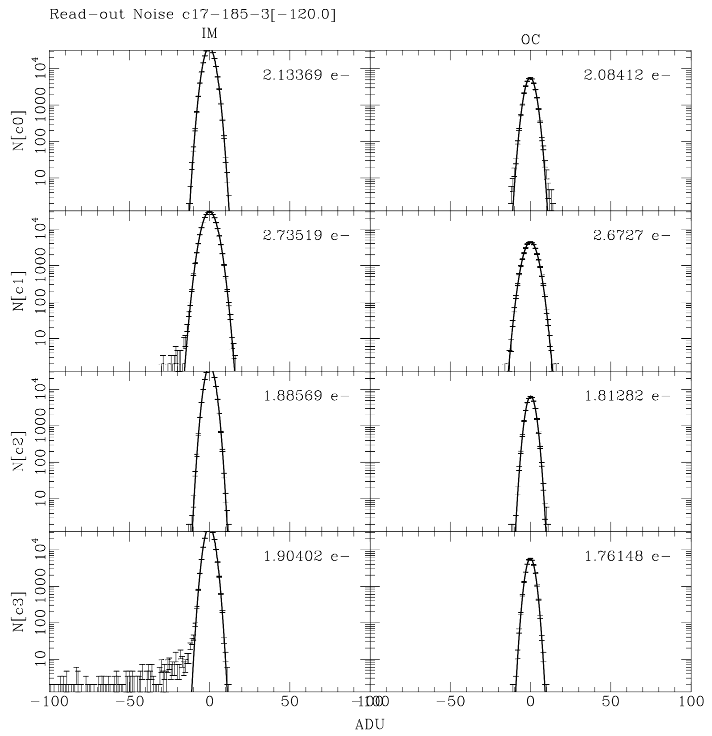

Figure 4 shows the data used in measuring the parallel CTI at 5.9 keV. Following Janesick, pulse height is plotted versus CCD row number, and a line of the form $ph(y) = ph(0) + \delta \cdot y$ is fit to the data.[7] Section 3.4 details this measurement.

The O K_α, Al K_α, and ^{55}Fe spectra from the same device are shown in figures 5, 6, and 7. The pulse heights range from 0 to 1700 ADU (analog-to-digital units) to permit a relative comparison of the spectral resolution at different energies. A consequence of each output having a different amplifier chain, and hence, a different gain is that the peaks occur at different ADU values for each node. The main oxygen peak lies at roughly 100 ADU. The higher energy features result from pile-up and non-suppressed 2nd and 3rd order photons produced by the monochromator. Besides the Mn K_α and Mn K_β lines, the ^{55}Fe spectra contains two other features. The line at about 1000 ADU is the Si K_α escape peak. The line at about 1300 ADU is a chromium fluorescence line produced when Mn X-rays scatter off the stainless steel vacuum tube of the test system.

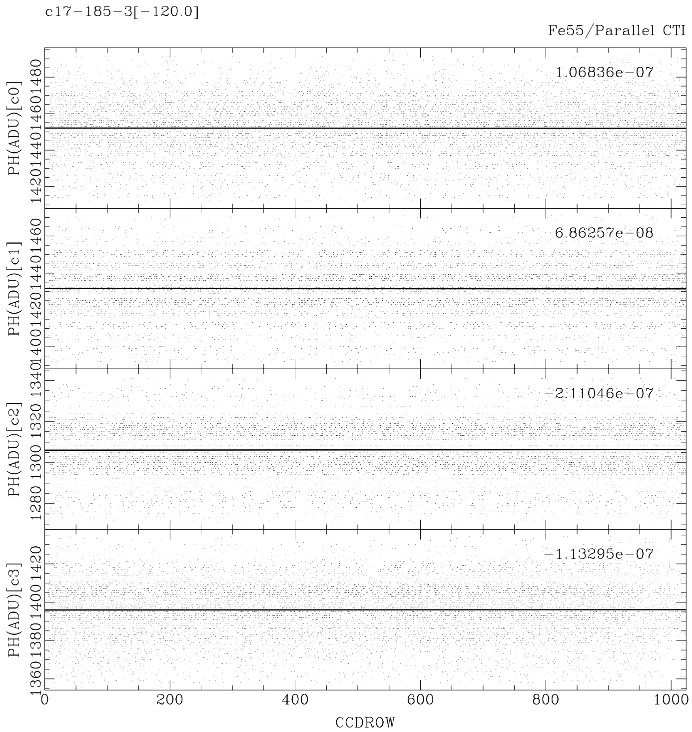

Figure 4: Parallel CTI determination from Mn K_α

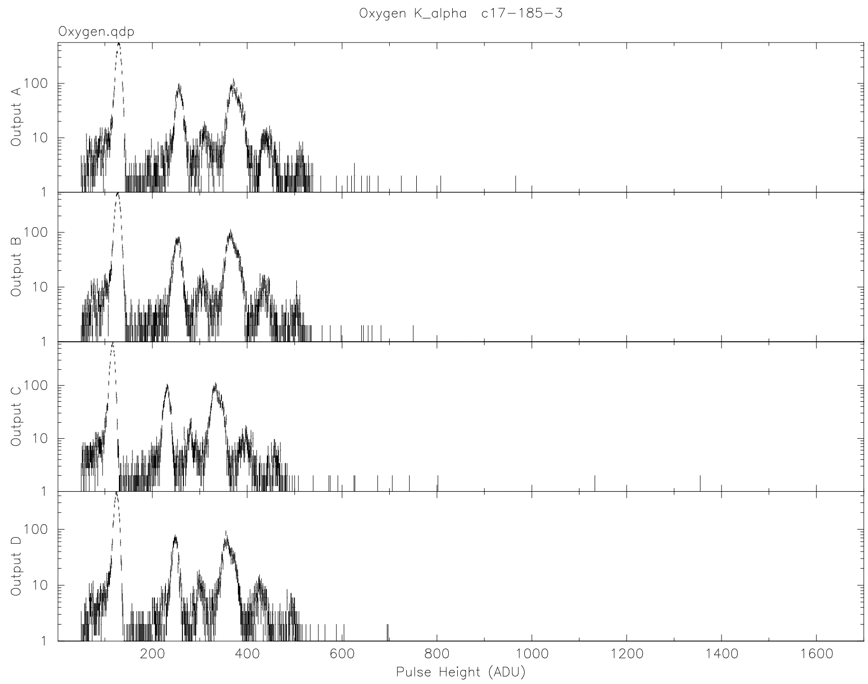

Figure 5: O K_α Spectra–525 eV

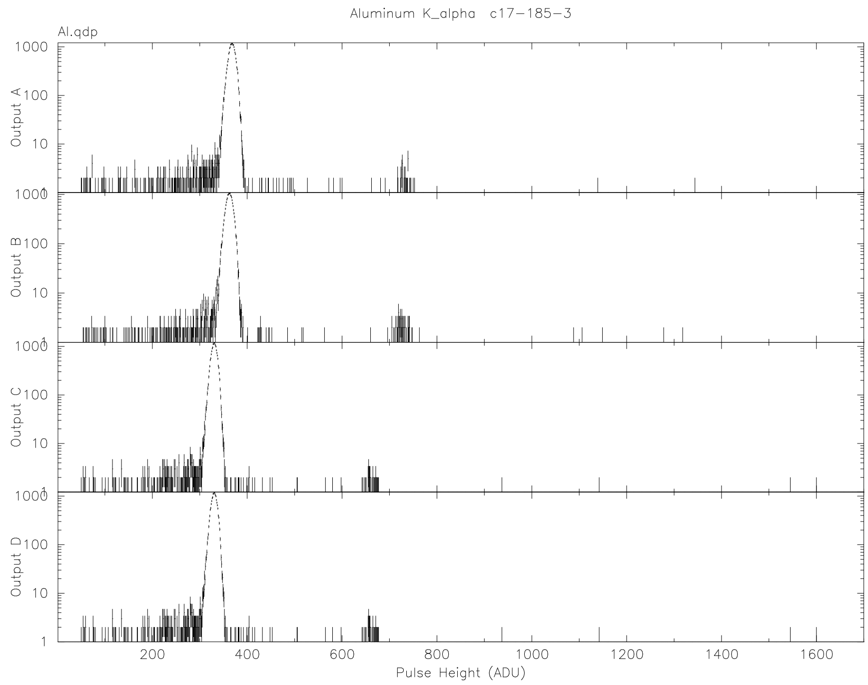

Figure 6: Al K_α Spectra–1.487 keV

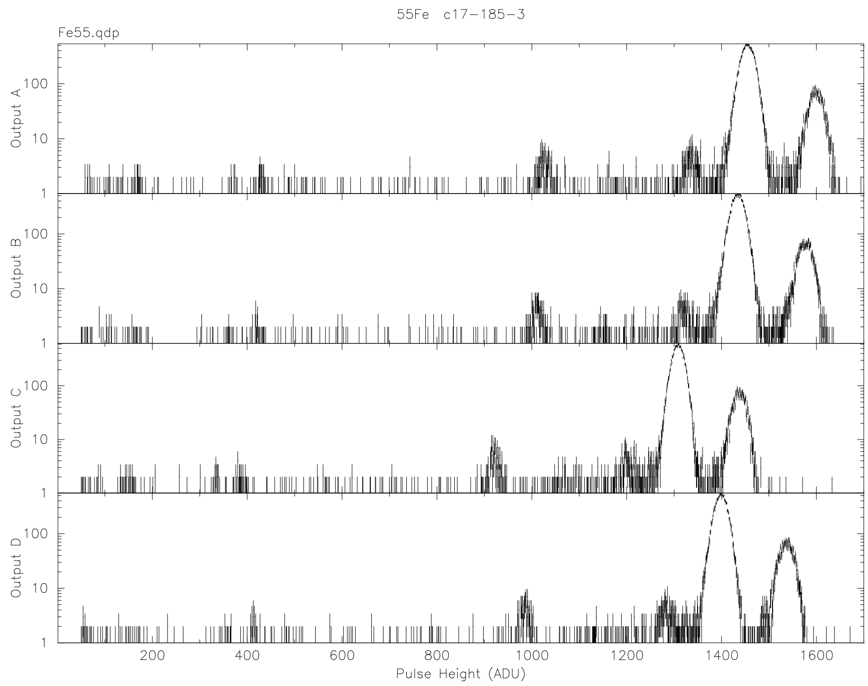

Figure 7: ^{55}Fe Spectra–5.898 keV

6 Conclusions

In order to efficiently use the limited time allotted for calibration of flight devices for the ACIS instrument, we have developed a screening protocol that measures device-level performance parameters. These measurements are then compared with the minimum acceptance criteria, allowing an informed decision to be made on whether to subject a CCD to a full calibration.

Most of the screened devices easily meet the acceptance criteria. On average a CCD will have RMS noise of 2-4 e^-, CTI below $1 \cdot 10^{-6}$, and spectral resolutions within 10 % of the theoretical limits. Given the uniformly high quality of the FI CCDs, we find that noise, low-energy (525 eV) spectral resolution and cosmetics are the most useful parameters for ranking devices.

7 REFERENCES

[1] A. Kenter, J. Gomes, S. Murray, R. Moore, R. Roll, M. Zombeck, "Testing Candidate MCPs for the AXAF HRC", *Proc. SPIE*, 2280, p. 69, 1995.

[2] T.H. Markert, C.R. Canizares, D. Dewey, M. McGuirk, C. Pak, M. L. Schattenburg, "The High Energy Transmission Grating Spectrometer for AXAF", *Proc. SPIE* , 2280, pp. 168-71 , 1994.

[3] D.H. Lumb, M.W. Bautz, J.P. Doty, G.P. Garmire, P. Gray, J.A. Nousek, G.R. Ricker, "Recent developments for the AXAF CCD Imaging Spectrometer", *Proc. SPIE*, 2006, pp. 265-271, 1993.

[4] B.E. Burke, R.W. Mountain, P.J. Daniels, M.J. Cooper, V.S. Dolat, "CCD Soft X-Ray Imagers for ASCA and AXAF", *Proc. SPIE*, 2006, pp. 278-284, 1993.

[5] M.W. Bautz, S. Kissel, G.Y. Prigozhin, S. Jones, T. Isobe, H.L. Manning, M. Pivovaroff, J. Woo, "X-ray CCD calibration for the AXAF CCD imaging spectrometer", *these proceedings.*

[6] R. van Grieken and A. Markowicz, *Handbook of X-ray Spectrometry*, Dekker, chs 3-4, 1993.

[7] J. Janesick, T. Elliott, R. Bredthauer, C. Chandler, B. Burke, "Fano-noise-limited CCDs", *Proc. SPIE*, 982, pp.70-95, 1988.